ELSEVIER

Polymer 43 (2002) 1375–1382

polymer

www.elsevier.com/locate/polymer

Slow crack propagation in polyethylene under fatigue at controlled stress intensity

V. Favier[a], T. Giroud[a], E. Strijko[a], J.M. Hiver[a], C. G'Sell[a,*], S. Hellinckx[b], A. Goldberg[c]

[a]*Laboratoire de Physique des Matériaux, UMR CNRS 7556, Ecole des Mines de Nancy (INPL), Parc de Saurupt, 54042 Nancy, France*
[b]*Research and Technology Center, Solvay, 310, rue de Ransbeek, 1120 Bruxelles, Belgium*
[c]*Solvay Polyolefins Europe, 310, rue de Ransbeek, 1120 Bruxelles, Belgium*

Received 12 July 2001; received in revised form 12 October 2001; accepted 18 October 2001

Abstract

Fatigue tests were performed on circumferentially notched bars (CNB) of high density polyethylene in order to analyse the kinetics and mechanisms of crack propagation. Tests were performed at 80 °C in order to accelerate the processes. Unlike standard fatigue procedure in which the force amplitude is constant, the original system utilised in this work was capable of imposing a constant stress intensity amplitude, K^{max}, during the whole propagation range. This was made possible through the real-time monitoring of crack propagation, $a(N)$, by means of a video-controlled technique. The results of the tests, for K^{max} in a range from 0.2 to 0.45 MPa $m^{1/2}$, show that stress intensity is the proper variable which controls crack propagation rate since, on the overall, crack speed is constant at constant K^{max} and no self-acceleration is observed unlike under force control. The empirical Paris law is verified under all conditions, with a stress intensity exponent close to 4. However, it is shown that constant crack speed is obtained only for $K^{max} < 0.25$ MPa $m^{1/2}$, when propagation proceeds through the continuous stretching and breaking of microfibrils in the localised craze at the tip of the crack. By contrast, at larger K^{max}, it is observed that crack tip successively jumps across the extended crazed zone in which very coarse fibrils were previously stretched from voids nucleated in the plane of maximum normal stress at a long distance ahead of the crack tip. © 2001 Published by Elsevier Science Ltd.

Keywords: Polyethylene; Fatigue; Video control

1. Introduction

Polyethylene is commonly used for the fabrication of gas or water pipes, in pressurised and non-pressurised applications. One of the most dangerous ruptures that a pipe may undergo is what is called failure by 'stress cracking'. This kind of failure occurs at long times and relatively low stresses after a crack has been initiated from a material inhomogeneity (microvoid, crystalline defect, aggregation of fillers, etc.) or from a macroscopic flaw caused by an accidental indentation. Its growth can lead either to a leak (slow crack growth) or to a catastrophic rapid crack propagation, depending on the service conditions and the design of the pipe.

Many progresses were accomplished the last decade to improve the performances of polymeric structures, especially through the development of new polyethylene grades more resistant to slow crack growth [1–3]. Consequently, there is an urgent need in finding a reliable test capable to assess quantitatively the crack growth kinetics and to optimise the material. Furthermore, since the sensitivity of polyethylene to processing conditions is rather high, such a test should be applicable to samples prepared either from compressed sheets or for pipe walls in order to separate the intrinsic properties of the material from the artefacts due to processing. Moreover, the initiation and propagation of the crack should occur within a reasonably short time. Lastly, the results of the test should be presented in such a way that they were exploitable for failure prediction in industrial cases.

In order to accelerate failure processes, many tests were imagined, in a wide variety of sample geometry, testing temperature, and environmental medium. However now, there is considerable scatter among these data and a lack of correlation with the results of tests performed on pipes. This is essentially because the phenomenon of plastic deformation and damage which arises in a pipe undergoing slow crack growth is not fully understood, so that it is difficult to reproduce it in different specimen types and/or for different loading histories. For example, it is difficult to reproduce in a simple laboratory test the multiaxial stress field induced in the pipe wall by an internal pressure, which

* Corresponding author. Tel.: + 00-33-383-584154; fax: + 00-33-383-579794.
E-mail address: gsell@mines.u-nancy.fr (C. G'Sell).

0032-3861/02/$ - see front matter © 2001 Published by Elsevier Science Ltd.
PII: S0032-3861(01)00701-7

leads to voids and crazes and/or shear bands, depending on the deformation processes that have been activated. Nevertheless, several authors have recently analysed this general problem with more realistic arguments than in the past [4–6], particularly by taking account of the influence of polymer viscoplasticity in the rupture criteria [7,8].

In this work, accelerated stable crack propagation was obtained by fatigue loading in notched polyethylene copolymer samples machined from compressed plates. The aim of the investigation is to study qualitatively and quantitatively the elementary processes which may cause failure in pressurised pipes subjected to long term loading: (i) slow crack propagation kinetics, (ii) damage mechanisms at the crack tip, and (iii) plastic deformation and damage of the polyethylene. Special attention is paid on the transition between continuous and discontinuous propagation pointed out 15 years ago by several authors in polymers from microfractographic observation [9,10], and revisited more recently by Brown and colleagues [11,12] in polyethylene under fatigue loading.

The original testing method developed for the present investigation is based on the video-controlled system (VidéoTraction™) initially set up at the Ecole des Mines of Nancy for uniaxial tensile tests [13]. It was adapted to measure crack propagation during fatigue cycling, with direct measurement of the crack length. Real-time control of propagation is based on the current value of stress intensity, K, considering that the assumptions of linear elastic fracture mechanics (LEFM) apply under plane strain conditions. The main features of the new fatigue testing procedure are presented in details and the results with polyethylene samples are analysed for different loading conditions at a single temperature chosen to promote crack propagation in a much shorter time than at room temperature.

This paper presents the macroscopic and microscopic aspects of slow crack growth in polyethylene. Particular attention is paid to the continuous vs. discontinuous nature of crack propagation. Crack growth rate data are analysed through Paris plots in terms of stress intensity, thus opening the way toward quantitative predictions. Multiscale morphological characterisation is finally performed in order to identify damage mechanisms at crack tip.

2. Experimental procedure

2.1. Material and fatigue specimen

The polyethylene investigated here is an experimental ethylene–butene copolymer from Solvay. It is a Ziegler-type grade of the second generation, designed for tubing with applications in medium-pressure gas, pressurised water and industrial fluids. The molecular weight distribution, determined by GPC, is characterised by $\bar{M}_n = 9152\ \mathrm{g\ mol^{-1}}$ and $\bar{M}_w = 236,094\ \mathrm{g\ mol^{-1}}$. It is coloured by about 2.5% of carbon black. The density of the pellets is equal to $955\ \mathrm{kg\ m^{-3}}$. The material was processed by compression moulding in the shape of 15 mm thick plates and cooled to room temperature at $15\ ^\circ\mathrm{C\ min^{-1}}$. The final degree of crystallinity, determined by differential scanning calorimetry using a conventional procedure, is equal to $58 \pm 3\%$ in weight.

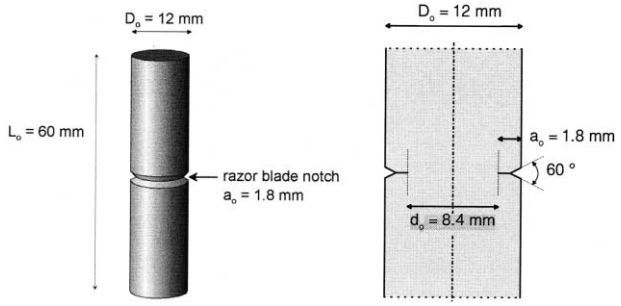

Fig. 1. Circumferentially notched bar specimen utilised in the fatigue tests. (general view and detailed view of the centre).

Following a strategy proposed by Solvay, the preference for fatigue testing was given to circumferentially notched bars (CNB) prepared from the polyethylene plates in the geometry shown in Fig. 1. The overall cylinder is machined on a lathe with a diameter, $D_o = 12$ mm and a length, $L_o = 60$ mm. An axisymmetric notch, 1.4 mm in depth, is then formed with a V-shaped tool in the median plane. Furthermore, the bottom of the notch is deepened very carefully on the lathe with a fresh medical scalpel, in such a way that the mechanical defect susceptible of stress cracking during the fatigue test has an initial depth, $a_o = 1.8$ mm exactly. The diameter of the material ligament remaining in the plane of the notch is thus equal to $d_o = 8.4$ mm.

2.2. Loading method, crack length measurement and crack tip profile examination

Fatigue tests were applied to the CNB specimens with a servo-hydraulic testing machine (Instron 8500) under square-shaped loading at a frequency of 1 Hz and at a temperature of 80 °C. This temperature was specifically chosen for it corresponds to the 'Notched Pipe Test' commonly used for tube failure characterisation [14]. Both minimum and maximum forces are positive, with a ratio, $R = F_{min}/F_{max}$, fixed at a value of 0.1. The 'net stress' in the ligament, defined as $\sigma = 4F/\pi d^2$, varies between σ^{min} and σ^{max} within each fatigue cycle, with a ratio also equal to 0.1. This tension–tension loading mode is severe enough to induce slow crack growth while avoiding specimen buckling and crack surface squeezing. Particular care was taken to optimise the axial alignment of the applied force.

The preference was given to the CNB specimens and not to the compact tension (CT) specimens for the following complementary reasons that (i) the geometry is very simple and is obtained with a single machining technique, (ii) the

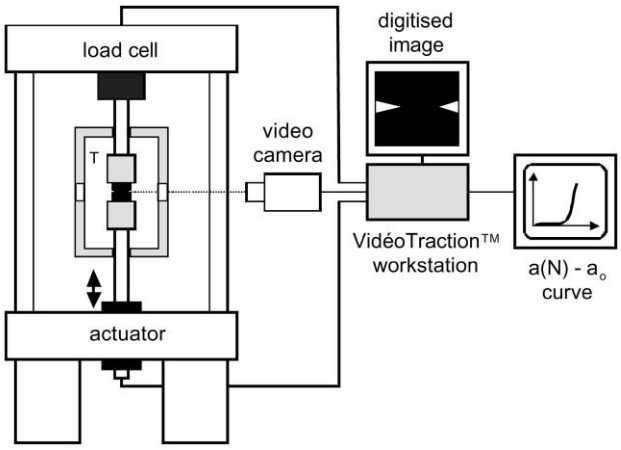

Fig. 2. Video-controlled fatigue testing system.

initial notch is applied very smoothly which is favourable for optimum crack initiation, (iii) the crack profile can be monitored throughout the whole test without any problem of concavity which would hide the actual crack tip, and (iv) the plane strain condition is relatively well defined in the ligament, as we will see later. For these reasons, the CNB specimens are good candidates to reproduce the long-term failure mechanisms of pipes.

The VidéoTraction™ system was first developed in order to control neck growth in hourglass shaped specimens of ductile materials under uniaxial tension [13], by means of a video camera interfaced with a microcomputer (Fig. 2). Here, during the fatigue tests, this system is utilised to analyse the profile of the notched specimens under rear illumination. Images are captured in real time every five cycles at the maximum stress plateau. At that moment, the crack is fully opened and appears in white with a good contrast with the material in black. The fast image processor detects the extreme white points at the crack tip on each side of the specimen profile and calculates the current diameter of the ligament, d, as the radial distance between these two points. For this measurement, the calibration of the image scale is performed from the calibrated diameter of the ligament, d_o, resulting from the scalpel indent. The initial crack length, $a_o = (D_o - d_o)/2$, is assessed during the first fatigue cycle as stress passes its maximum. Providing that the propagation of the crack is symmetrical (this is checked systematically), the crack length after N fatigue cycles is defined as $a(N) = [D_o - d(N)]/2$ where D_o, the overall diameter, does not change significantly as crack propagates. The rate of crack growth per cycle, conventionally written as da/dN, is measured from the $a(N)$ records through the ratio $\Delta a/\Delta N$, where Δa is the increase in the crack length over an increment of cycle number, ΔN. Considering the quality of the propagation curves obtained in this work, the value of $\Delta N = 300$ corresponds to the best compromise since it smoothens the noise without loosing the significant details of the kinetics. This notion of 'incremental slope' is similar to the approach of Zhou and Brown [15].

2.3. Dynamic control of stress intensity

In the case of a circumferentially notched specimen, Murakami and Nisitani [16] derived the expression of stress intensity under the linear elastic (LEFM) assumptions. It writes in the general form: $K = \Sigma \times (\pi a)^{1/2} \times Y(a, D)$, where Σ represents the bulk stress far from the notch and Y a dimensionless geometrical factor. For the CNB specimen, $D \approx D_o$ (no deformation in the bulk), and consequently $\Sigma = \Sigma_o = 4F/\pi D_o^2 = \sigma_o d_o/D_o$. In those circumstances, $Y(a, D) = Y(a, D_o)$ is given by the following equation of Murakami and Nisitani:

$$Y(a, D_o) = \frac{1.121 - 3.08(a/D_o) + 7.344(a/D_o)^2 - 10.244(a/D_o)^3 + 5.85(a/D_o)^4}{[1 - 2(a/D_o)^2]^{3/2}} \quad (1)$$

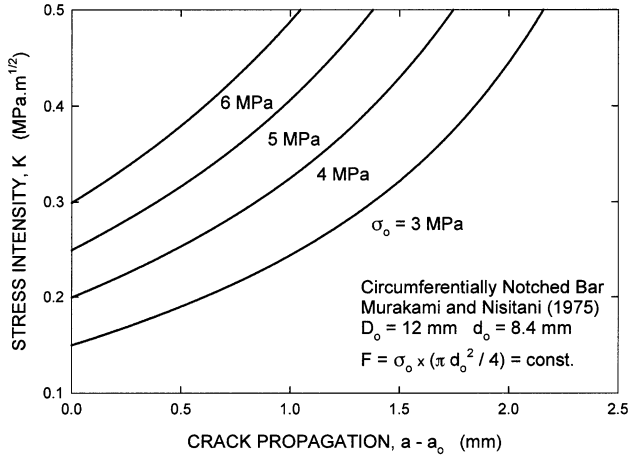

Fig. 3. Evolution with crack length of stress intensity under a constant force corresponding to given values of σ_o (after Murakami and Nisitani [16]).

After these authors, this expression of $Y(a/D_o)$ is valid over the whole propagation range, $(0 \le (a/D_o) \le 0.5)$ and approximates the stress intensity better than 1%. In the CNB specimen sketched in Fig. 1, the influence of crack propagation on stress intensity is displayed in Fig. 3 for different values of $\sigma_o = 4F/\pi d_o^2$ (that is for different values of the applied force).

In the present work, the experimental apparatus is capable of running the fatigue tests in two contrasting ways: (i) either under force control, with F^{min} and F^{max} being constant whatever the crack length (the F values being chosen to fit given values of σ_o), or (ii) under stress intensity control, the force signal being readjusted every five cycles as a function of the current crack length in such a way that K^{min} and K^{max} remain constant along successive cycles until the specimen breaks. In both control modes, the ratio $R = \sigma_o^{min}/\sigma_o^{max} = K^{min}/K^{max}$ is kept equal to 0.1.

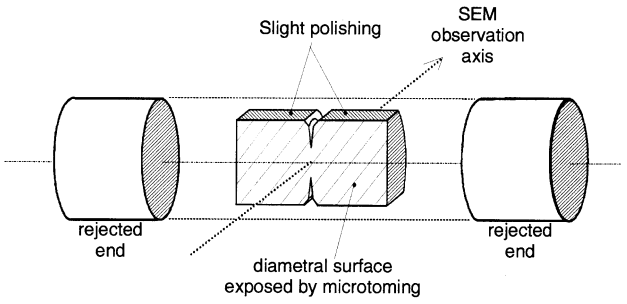

Fig. 4. Sample cut into the specimen by microtoming for SEM observations.

2.4. Sample preparation for microscopic characterisation

In order to investigate the microstructure at crack tip in course of propagation before the specimen is totally fractured, some tests are interrupted at a predefined crack length and the force is held at a precise level corresponding to $K_{max}/2$, in order to stop the growth of the crack while maintaining it partially open. The specimen is quenched down to room temperature by means of a nitrogen spray in such a way that the molecular mobility is reduced and the current microstructure of the material is frozen. The specimen is then truncated by removing successive slices with a Leitz microtome until reaching the diametral plane of the cylinder, as sketched in Fig. 4. This technique allows a fine observation of the crack since it does not affect significantly the microstructure unlike polishing techniques. The prepared surfaces are gold-sputtered and analysed with a JEOL 820 scanning electron microscope (SEM). In this procedure, it is important to prepare and observe the specimen as quick as possible (a few hours after the interruption of the fatigue test) in order to avoid extensive relaxation of the polymer and the closing back of the crack. It is thus possible to characterise the damage undergone by the polymer at the tip of a crack whose length was precisely measured by the video-controlled system.

3. Crack propagation kinetics

3.1. Fatigue tests under force control

The evolution of crack length under force control is illustrated in Fig. 5 for σ_o^{max} ranging from 3.5 to 5 MPa. It is interesting to note that the four curves display the same qualitative features with three successive stages which are interpreted from the crack tip images monitored by the VidéoTraction™ system during the test. In the *incubation stage*, which varies from about 26,000 cycles for $\sigma_o^{max} = 5$ MPa to about 150,000 cycles for $\sigma_o^{max} = 3.5$ MPa, the crack length experiences a very limited variation (less than 0.1 mm), resulting of the blunting of the initial notch. In the *propagation stage*, a fine crack is formed at the tip of the blunted notch, and grows more and more rapidly. In the

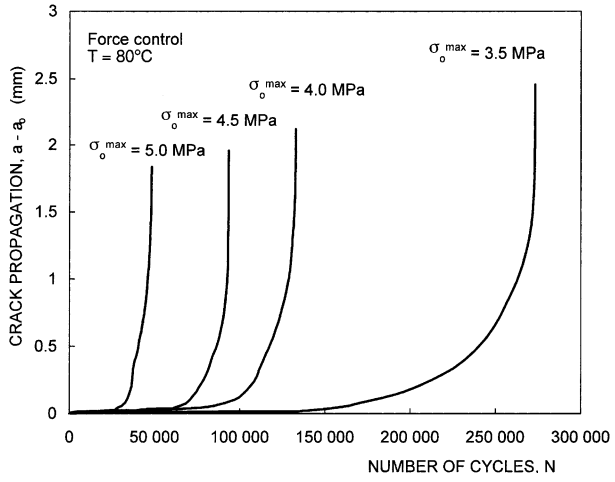

Fig. 5. Influence of the initial net stress on crack propagation kinetics under load control.

termination stage, one notes a very fast increase of da/dN, ending by the brutal fracture of the specimen along the propagation plane for a total 'fatigue life' ranging from 47,600 cycles (that is about 13 h) to 275,000 cycles (more than 76 h). The propagation stage described above is typical of the so-called 'slow crack growth' regime described by several authors (e.g. Ref. [9]).

A comment should be made concerning the experiment at $\sigma_o^{max} = 5$ MPa. This upper bound of the stress is dictated by the limited yield stress of the polyethylene at 80 °C ($\sigma_y = 5.5$ MPa at a strain rate of $5 \times 10^{-5}\ s^{-1}$ and $\sigma_y = 8.5$ MPa at $5 \times 10^{-3}\ s^{-1}$) so that as the net stress σ increases in the ligament, more plastic flow occurs at the crack tip. However, despite the rather high value of the net stress, plastic yielding does not spread over the whole cross section because: (i) the ligament is subjected to plane strain tension under which yield stress is higher than in uniaxial tension, and (ii) the strain rate experienced by the material during a fatigue cycle is higher than $10^{-2}\ s^{-1}$ (even including the 0.5 s holding time at the stress plateau).

3.2. Fatigue tests under stress intensity control

The kinetics of crack propagation under stress intensity control is studied in a range from $K^{max} = 0.2$ to 0.45 MPa $m^{1/2}$. A series of five experiments under stress intensity control is displayed in Fig. 6. As for the experiments under force control, these fatigue tests exhibit an initial incubation stage until crack growth is initiated. However, a striking feature is observed in the propagation stage: instead of exhibiting a gradual increase in the propagation rate, the $a(N)$ curves at constant K^{max} are almost linear. Consequently stress intensity can be considered as the driving force of slow crack propagation since tests at constant K^{max} lead to crack propagation at constant da/dN. Moreover, termination stage is not visible any longer since,

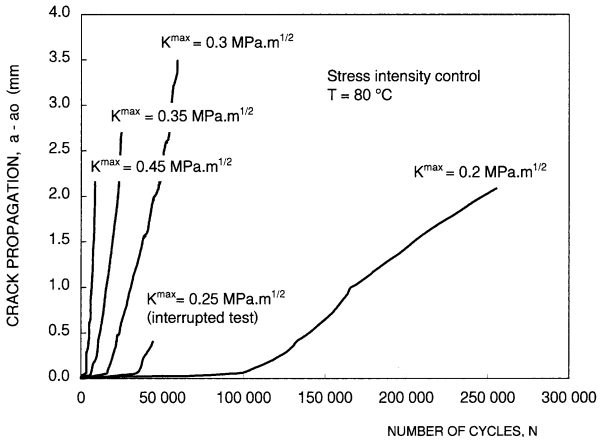

Fig. 6. Influence of the stress intensity on crack propagation kinetics under stress intensity control.

unlike in tests under force control, $K^{\max}$ does not increase with crack length.

A more detailed analysis of the curve reveals that the crack growth rate stability (smoothness of the curves) depends on the value of $K^{\max}$: crack propagation at low stress intensity is much more stable than those at high stress intensity which grow by successive steps as we shall examine later in more details from the mesoscopic observation of crack tip. The transition from continuous to discontinuous crack propagation is between $K^{\max} = 0.2$ and 0.3 MPa $m^{1/2}$.

3.3. Application of Paris propagation law

The quantitative modelling of crack propagation in materials under fatigue has been the object of much effort in the past due to the necessity of predicting long term service lives under stresses lower that those compatible with experimental times. Like for metallic materials, many authors have shown that, in polymers, stress intensity constituted a leading parameter controlling the propagation rate [10,12,17–22]. In particular, they showed that the variations of da/dN in fatigue could be correctly represented in terms of stress intensity through the Paris empirical power law

$$\frac{da}{dN} = A\,\Delta K^m \tag{2}$$

where $\Delta K = K^{\max} - K^{\min} = K^{\max}(1 - R)$ is the amplitude of the stress intensity fatigue signal, while A and m are constants depending on the material and the testing conditions but without any physical meaning.

In all previous papers dealing with crack propagation modelling, the parameters A and m of the Paris law were determined by analysing the variation of da/dN vs. ΔK in a double log plot, which should fit a linear regression of slope m. Since these studies were based on fatigue tests under force control, the value of ΔK increases gradually as crack propagates, so that a whole Paris plot could be obtained in principle from only one experiment. This procedure can be considered as an advantage since it minimises the experimental investment. However, it does not guarantee that da/dN depends on ΔK only, since the variation of crack length during the test could be suspected to have its own influence.

We have the advantage, with the system used for present study, to choose the control mode and to work either at constant ΔF or at constant ΔK. In order to analyse the dependence of da/dN on ΔK, all experimental data are exploited such as the $a(N)$ curves of Fig. 5 at constant ΔF, and $a(N)$ curves of Fig. 6 at constant ΔK. From the former set of data, according to literature [9,23], we systematically eliminated the points corresponding to the foot of the curves (initiation stage) and the ultimate acceleration (rupture stage) and kept only the data corresponding to the stable crack growth stage. In the plot of Fig. 7, these data are plotted in a (log da/dN) vs. (log ΔK) graph with four open symbols corresponding to four values of ΔF corresponding to initial maximum stresses, $\sigma_o^{\max}$, ranging from 3.5 to 5.0 MPa. With this plot, we confirm the conclusion of previous authors [9,10,12,20–25], that crack propagation obeys well the Paris law, with a correlation factor of 0.9855. The scaling factor, determined from this logarithmic regression, is thus equal to $A = 7.1 \times 10^{-3}$ (for units of mm/cycle and MPa $m^{1/2}$). As for the exponent, it is equal to $m = 3.82$, in good agreement with literature which agrees on values of m near 4.0.

Let us consider now the plots with filled squares in Fig. 7 corresponding to fatigue tests at constant ΔK (four values equal to 0.2, 0.3, 0.35 and 0.45 MPa $m^{1/2}$, respectively). Since we noted that crack propagation was sometimes rather jerky, the propagation rate, da/dN, suffers some fluctuations whose standard deviation is indicated with error bars attached to the plot of the average rate. It is interesting to remark that the results of tests at constant ΔK align with the same regression line as the tests at constant ΔF, within the limits of experimental errors. As suggested before by Chan

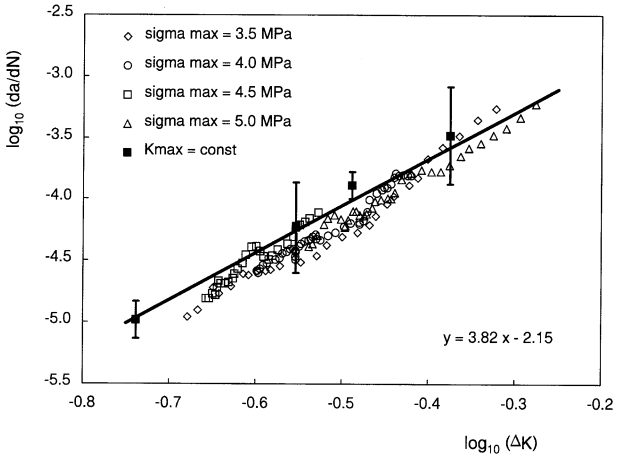

Fig. 7. Paris plot of the stable crack propagation data for the fatigue tests at constant ΔF (open symbols) and at constant ΔK (filled symbols). Units are: MPa $m^{1/2}$ for ΔK, and mm/cycle for da/dN.

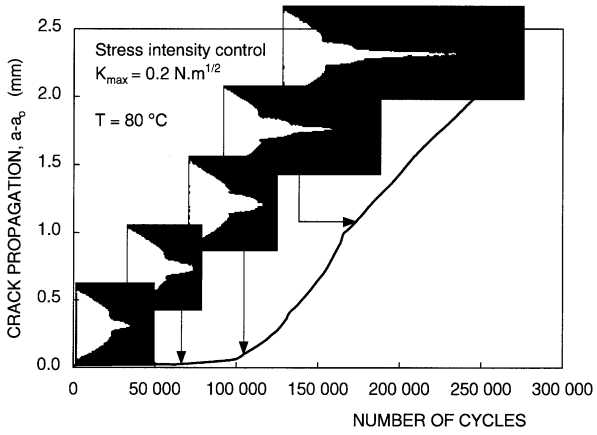

Fig. 8. Crack propagation kinetics and profiles for a fatigue test under stress intensity control at $K_{max} = 0.2$ MPa m$^{1/2}$.

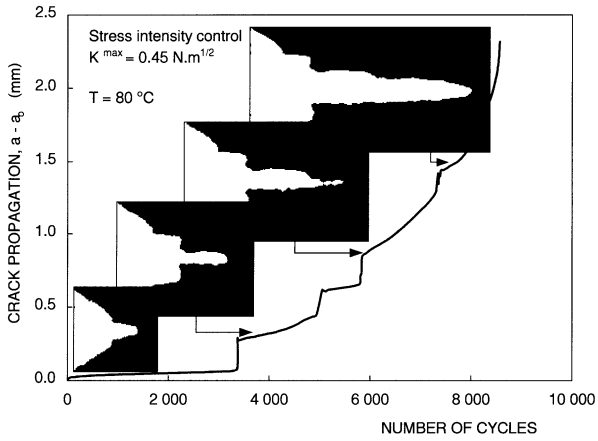

Fig. 9. Crack propagation kinetics and profiles for a fatigue test under stress intensity control at $K_{max} = 0.45$ MPa m$^{1/2}$.

and Williams [9], this work shows that propagation rate depends essentially on stress intensity and not on the mechanical history of the crack. Furthermore, it shows that the Paris law, although empirical, is operationally adapted to describe crack propagation kinetics in this kind of polyethylene under fatigue. This result was not obvious a priori since some of the tests are performed for stresses in the ligament close to yield stress, so that it might be suspected that LEFM (from which the notion of stress intensity comes) is not strictly applicable. The good agreement of experimental data with a single set Paris parameters is an indication that the crack propagation process is dominated by the slow crack growth mechanisms in the entire ΔK range considered in this work.

4. Multiscale microstructural investigation

4.1. In situ mesoscopic observation of crack tip profiles

A particular feature of the experimental procedure designed for this work is to give access in real time to the shape of the crack tip on the control monitor of the system. The images can thus be recorded at time intervals for pre-set values of crack propagation for further exploitation. We now discuss such results for two typical experiments run under two contrasting values of maximum stress intensity: $K^{max} = 0.2$ and 0.45 MPa m$^{1/2}$, respectively.

In the test at $K^{max} = 0.2$ MPa m$^{1/2}$ (Fig. 8), the very long incubation period (lasting about 100,000 cycles) shows moderate blunting of the original razor blade notch and very limited increase of the notch length (due to general viscoelastic deformation of the specimen). Subsequently, the propagation stage begins through the initiation of a very thin crack at the bottom of the notch and the very regular propagation of this crack, over a distance more than 2 mm, at a nearly constant rate $da/dN \approx 1 \times 10^{-5}$ mm/cycle.

For the experiment at $K^{max} = 0.45$ MPa m$^{1/2}$ (Fig. 9), the incubation period is much reduced, about 3380 cycles. Blunting is much more important than at low stress intensity. This process, which has been discussed in details by several authors [9–11,26–29] has been ascribed to the formation of a zone of intense deformation at the tip of the notch, usually called 'plastic zone'. Here again, crack propagation begins through the initiation of a thin crack at the notch bottom of the blunted notch, but unlike at low K^{max} the crack jumps suddenly over a distance of about 0.25 mm. Then, a stage of slow propagation begins for about 1500 cycles during which the crack tip blunts again. Successive sequences of crack jumping and crack blunting are successively observed in the $a(N)$ curve during the rest of the test, giving to it a typically step-like aspect which has already been mentioned in the literature and has been studied for different kinds of tests (fatigue, creep) [9,10,30–32].

4.2. Microscopic characterisation of the plastic zone

Scanning electron micrographs of polyethylene sections across the tip of fatigue cracks are obtained at different stages of their propagation under various stress intensity levels. Although these micrographs are not observed in situ while the test is running, the experimental procedure which is utilised guarantees that no serious perturbation has affected the material during the quenching, unloading, and microtoming operations, so that the microstructural features revealed by the SEM can be regarded as representative of the current state of the crack during the propagation.

The first results refer to a specimen fatigued under 'low' stress intensity amplitude ($K_{max} = 0.2$ MPa m$^{1/2}$), that is for continuous propagation at nearly constant da/dN. The micrograph of Fig. 10(a) shows a very thin crack after a propagation for about 160,000 cycles over a distance of 0.9 mm. The crack trajectory is almost straight and close to the plane of maximum normal stress. At a higher magnification (Fig. 10(b)), one notes that the crack lips are covered by a dense collection of broken microfibrils. Some of them are grouped in entangled bundles. Near the

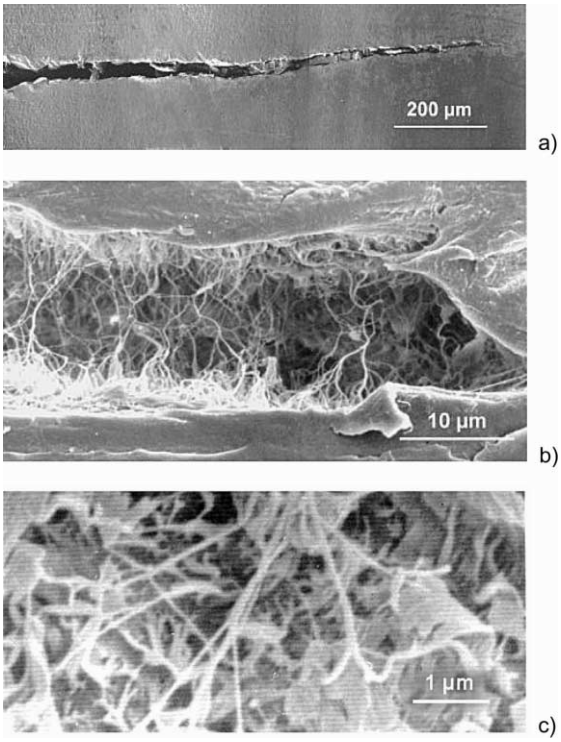

Fig. 10. Observation of a fatigue crack under continuous growth regime for $K_{max} = 0.2$ MPa $m^{1/2}$: (a) overall view of the crack, (b) observation of microfibrils, (c) enlarge view of microfibrils near crack tip.

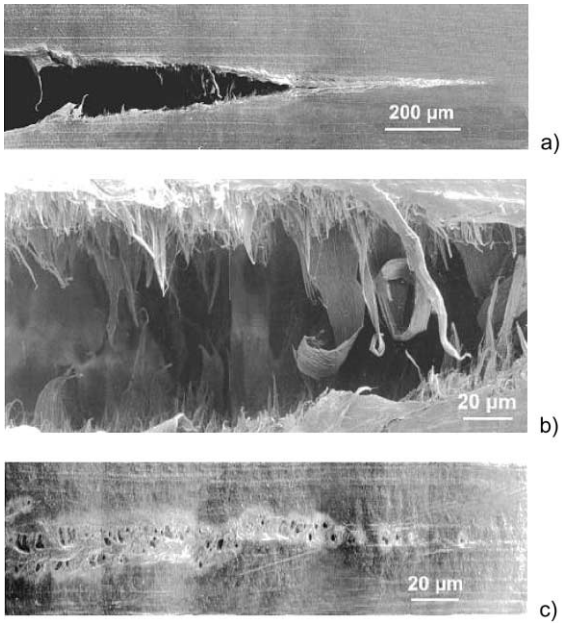

Fig. 11. Observation of a fatigue crack under discontinuous growth regime for $K_{max} = 0.3$ MPa $m^{1/2}$: (a) overall view of the crack, (b) coarse microfibrils within the crack, (c) cavitation ahead of the crack tip.

crack tip, a definite craze zone is observed (over a distance of 20–30 μm), in which most microfibrils have been stretched but not broken (Fig. 10(c)). The elementary fibrils are extremely fine, about 50–100 nm in diameter. As for the material ahead of the crack, careful examination of the electron micrographs shows no evidence of damage. Since the tip of the crack is very acute, it is probable that plastic deformation is very limited. All the above features show that crack growth under low stress intensity results on: (i) the continuous formation of a very confined craze at the crack tip within undamaged polyethylene, (ii) the overstretching of microfibrils until their diameter is reduced down to nanometric dimensions and, (iii) the ultimate rupture of the microfibrils allowing the opening of the crack in region behind the craze.

The above results are now compared with micrographs obtained after about 30,000 fatigue cycles under 'high' stress intensity amplitude ($K_{max} = 0.3$ MPa $m^{1/2}$), that is after the discontinuous (step-like) propagation of the crack over a distance of about 0.6 mm. The micrograph of Fig. 11(a) shows the general features of the crack. Near the left side of the image, one notes the position of the original razor blade notch, which was considerably blunted during the incubation stage. Just on the right of this notch one observes the open crack, whose extremity corresponds to the 'crack tip' position recorded by our video-controlled testing system. It is interesting to note that many debris of stretched fibrils collapsed on the crack lips. A detailed view of these fibrils, displayed in Fig. 11(b), shows that they are much coarser than under low stress intensity, their diameter being larger than 1 μm. Some of them appear like massive strips broken in their middle and sometimes at their extremities. Returning to Fig. 11(a), it is evident that the polyethylene is damaged ahead of the crack tip, principally along the plane of maximum normal stress. The damaged zone is visible in Fig. 11(a) over a distance as large as 600 μm. Careful examination of this zone shows, starting from the crack tip: (i) a dense craze over a distance of about 300 μm, (ii) a region with well-developed voids over the next 200 μm, (iii) a collection of tiny cavities with nanometric sizes over about 100 μm before reaching the sane material. The micrograph of Fig. 11(c) shows, at a higher magnification, the extreme right part of the damaged zone in which the cavities are clearly resolved. One should notice that the length of the jumps experienced by the crack at the discontinuities observed in the tests at high K_{max} (e.g. in Fig. 9) are of about 200 μm, of the same order as the crazed zone ahead of the crack tip. It is thus likely that the formation of the craze at the crack tip is the precursory mechanism of the forthcoming propagation step.

5. Conclusions

An original video-controlled testing method has been designed for monitoring and controlling crack propagation in CNB of polyethylene during fatigue testing. This technique shows its capacity to provoke early nucleation of slow crack propagation within a reasonably short time. It is utilised for controlling crack growth: (i) under force control

and, (ii) under stress intensity control. In the former control mode, the propagation rate is self-accelerated, while no acceleration is recorded in the latter mode. However, when the crack propagation is followed in details, it is noted that crack speed is more or less constant according to the applied stress intensity amplitude and in relation with microstructural features. In the range for $K^{max} < 0.25$ MPa $m^{1/2}$, the crack is very thin and grows in a quite continuous way. The crazed zone at the crack tip is very limited, and crack propagation proceeds through the progressive overstretching and breaking of very thin microfibrils in this craze. By contrast, for $K^{max} > 0.25$ MPa $m^{1/2}$, crack propagates through a succession of jumps and arrests. Microscopic observation shows that this discontinuous growth results on a series of complex mechanisms taking place within an extended damaged zone in the plane of maximum normal stress ahead of the crack. These mechanisms involve cavitation, voiding, coarse fibril formation and rupture.

Whatever be the crack propagation mechanisms, it is shown that the incremental crack speed obeys the empirical Paris law, $da/dN = A\Delta K^n$ is correctly verified. This indicates that, on average, the propagation rate depends on the instantaneous state of stress at the crack tip. The influence of mechanical history seems only limited to discontinuous growth phenomena under large K^{max}, when the crack tip jumps over the length of the crazed zone which slowly formed during the preceding crack arrest time. Prediction of flaw behaviour and safe lifetime of polyethylene structures (like gas or water pipes) can be envisaged on the grounds of the above mechanisms. Further work will be devoted to this kind of prediction.

References

[1] Böcker H, Dewitt R. High performance PE provides better safety for pipelines. Kunststoffe 1992;82:739–43.

[2] Dewitt R. High performance PE compounds for safer gas and water transportation. Plastic Pipes 1992;VIII:C2/2.

[3] Ahlstrand LE, Le Roux D, Espersen H. PE100 opens new horizons for plastic pipes. Plastics Pipes 1998;X:9 Göteborg, Sweden.

[4] Rose L, Channell AD, Frye CJ, Capaccio G. Slow crack growth in polyethylene: a novel predictive model based on the creep of craze fibrils. J Appl Poym Sci 1994;54:2119–24.

[5] Boytard K, Kichenin J, Dang Van K. Characterisation and modelization of the slow crack growth mechanisms in the extruded PE pipes. Thirteenth International Plastic Fuel Gas Pipe Symposium. 1993. p. 291.

[6] Boytard K, Ouakka A, Dang Van K. A modelling tool for the mechanical behaviour of PE pipes. Second International Conference on Pipeline Technology, Ostend. 1995.

[7] Stojimirovic A, Kadota K, Chudnovsky A. An equilibrium process zone in polymeric materials. J Appl Polym Sci 1992;46:1051–6.

[8] Kadota K, Chudnovsky A. Constitutive equations of crack layer growth. Polym Engng Sci 1992;32:1097–104.

[9] Chan MKV, Williams JG. Slow stable crack growth in high density polyethylenes. Polymer 1983;24:234–44.

[10] Hertzberg RW, Manson JA. Fatigue of engineering plastics. New York: Academic Press, 1980. Chapter 3.

[11] Lu X, Quian R, Brown N. Discontinuous crack growth in polyethylene under a constant load. J Mater Sci 1991;26:917–24.

[12] Zhou Y, Brown N. The mechanism of fatigue failure in a polyethylene copolymer. J Polym Sci, Polym Phys Ed 1992;30:477–87.

[13] G'Sell C, Hiver JM, Dahoun A, Souahi A. Video-controlled tensile testing of polymers and metals beyond the necking point. J Mater Sci 1992;27:5031–9.

[14] ISO standard, EN 13479. Polyolefin tubes for conveyance of fluids—determination of resistance to crack propagation—test method for slow crack growth on notched pipes (notch test). 1997.

[15] Zhou Y, Brown N. A new automated method for recording and predicting failure by slow crack growth in polyethylene. Polym Testing 1996;15:549–58.

[16] Murakami Y, Nisitani H. Stress intensity factor for circumferentially cracked round bar in tension. Trans Jpn Soc Mech Engng 1975;41:360–9.

[17] Michel J, Manson JA, Hertzberg RW. Polymer 1984;25:1657.

[18] Bucknall CB, Dumpleton P. Factors affecting fatigue crack growth in HDPE. Plast Rubb Process Appl 1985;5:343–7.

[19] Dumpleton P, Bucknall CB. Comparison of static and dynamic fatigue crack growth rates in high-density polyethylene. Int J Fatigue 1987;9:151–5.

[20] Nishimura H, Narisawa I. Fatigue behaviour of medium-density polyethylene pipes. Polym Engng Sci 1991;31:399–403.

[21] Pruitt L, Hermann R, Suresh S. Fatigue crack growth in polymers subjected to fully compressive cyclic loads. J Mater Sci 1992;27:1608–16.

[22] Brown N, Huang LX, Qian R. Slow crack growth in polyethylene—a review. Makromol Chem, Macromol Symp 1995;41:55.

[23] Klesnil M, Lukas P. Influence of strength and stress history on growth and stabilisation of fatigue cracks. Engng Fract Mech 1972;4:77–92.

[24] Brown N, Lu X. A fundamental theory for slow crack growth in polyethylene. Polymer 1995;36:543–8.

[25] Brown N, Lu X. The fracture mechanics of slow crack growth in polyethylene. Int J Fract 1995;69:371–7.

[26] Lu X, Brown N. The relationship of the initiation stage to the rate of slow crack growth in linear polyethylene. J Mater Sci 1986;21:2423–9.

[27] Williams JG. Fracture mechanics of polymers. Chichester: Ellis Horwood, 1984.

[28] Brown N, Bhattacharya SK. The initiation of slow crack growth in linear polyethylene under single edge notch tension and plane strain. J Mater Sci 1985;20:4553–60.

[29] Strebel JJ, Moet A. Plane strain and plane stress analysis of fatigue crack propagation in medium density polyethylene pipe materials. Polym Engng Sci 1993;33:217–26.

[30] Duan DM, Williams JG. Craze testing for tough polethylene. J Mater Sci 1998;33:625–38.

[31] Shah A, Stepanov EV, Capaccio G, Hiltner A, Baer E. Stepwise fatigue crack propagation in PE resins of different molecular structure. J Polym Sci, Part B: Polym Phys 1998;36:2355–69.

[32] Kadota K, Chum S, Chudnovsky A. Bridging the PE lifetime under fatigue and creep conditions with its crystallization behavior. J Appl Polym Sci 1993;49:863–75.